ELSEVIER

Journal of Molecular Catalysis A: Chemical 155 (2000) 13–22

JOURNAL OF MOLECULAR CATALYSIS A: CHEMICAL

www.elsevier.com/locate/molcata

Reconstructive activation of bimetallic surfaces Catalytic reduction of NO with H_2 on Pt(100), Pt(110), Rh(100), Rh(110) and bimetallic single crystal surfaces of Rh/Pt(100), Rh/Pt(110), Pt/Rh(100), and Pt/Rh(110)

Ken-ichi Tanaka *, Akira Sasahara

The Institute for Solid State Physics, The University of Tokyo, 7-22-1 Roppongi, Minato-ku, Tokyo, 106 Japan

Received 20 September 1998; accepted 1 February 1999

Abstract

When Pt–Rh alloy or Pt/Rh bimetallic surfaces were exposed to O_2 or NO, Rh atoms underwent segregation at temperatures higher than ca. 400 K, and was followed by the characteristic restructuring. That is, Pt–Rh(100) alloy, Rh/Pt(100) and Pt/Rh(100) bimetallic surfaces commonly form a $p(3 \times 1)$ structure by heating in O_2, and Pt/Rh(110) and Rh/Pt(110) surfaces heated in O_2 give $c(2 \times 4)$ and $c(2 \times 2)$ LEED pattern, respectively. Interestingly, the catalytic activity of the bimetallic surfaces for $NO + H_2$ reaction was markedly enhanced by the reconstruction and became structure insensitive. An STM image in atomic resolution revealed an ordered Rh and Pt composite structure for the $p(3 \times 1)$ Pt–Rh(100)/O alloy surface. These results suggest that the reconstructed bimetallic surfaces may be composed of the active sites, having a common local structure.

Keywords: Pt/Rh(100) alloy; Rh/Pt(100) bimetallic catalyst; Pt/Rh(100) bimetallic catalyst; Pt/Rh(110) bimetallic catalyst; Rh/Pt(110) bimetallic catalyst; $NO + H_2$ reaction; Structure sensitive catalysis; STM image of activated Pt/Rh(100) alloy catalyst

1. Introduction

A catalytic reaction is composed of several elementary processes, and the slowest step(s) of them is responsible for the activity and the kinetic feature of catalysis. So far, the reaction mechanism in catalysis has been tacitly explained by assuming two-dimensional gas-like adsorbed species. However, we can now gain an insight into the surface structure in atomic level details so that the importance of the local structure of the active sites can be discussed.

How to get and how to design an optimized long life catalyst has been a long standing desire in the heterogeneous catalyst. In this respect, a very important result was presented by Bare et al. [1,2] in the ammonia synthesis reaction on single crystal Fe surfaces. It has been known that the catalytic activity of Fe single crystal surfaces for ammonia synthesis reaction is in a sequence of $Fe(111) \gg Fe(100) > Fe(110)$, that is, the catalytic activity of Fe single crystals is

* Corresponding author. Present address: Saitama Institute of Technology, Okabe, Saitama, Japan. Tel. + fax: +81-48-585-6874.
E-mail address: ktanaka@sit.ac.jp (K. Tanaka).

1381-1169/00/$ - see front matter
PII: S1381-1169(99)00315-5

quite sensitive to their crystallographic surface structures. On the other hand, Al_2O_3 is one of the indispensable promoting materials in the industrial Fe catalyst, but the role of Al_2O_3 has still not been clear. Bare et al. found that the catalytic activity of Fe(100) and Fe(110) is markedly enhanced when the surface is covered with a $FeAl_2O_4$ over-layer, and they supposed from the TPD experiments that a Fe(111) like over-layer may grow on the $FeAl_2O_4$ layer during heating in a mixture of $N_2 + H_2$ at 673 K. That is, Fe(100) and Fe(110) surface are activated by a chemical restructuring forming $FeAl_2O_4$ layer and the growth of (111) like overlayer on it. It is noteworthy that it is still an unsolved interesting question why Fe(111) is so active for ammonia synthesis reaction.

Similar activation of the surface by chemical restructuring has been observed on Pt/Rh alloy, as well as on Pt/Rh bimetallic surfaces [3,4]. It is well known that Pt/Rh bimetallic catalyst is a prominent catalyst for NO_x reduction in the exhaust gas of gasoline automotive, but the role of Rh is still not clear. When a $p(1 \times 1)$ $Pt_{0.25}Rh_{0.75}(100)$ alloy surface was heated in NO or O_2, Rh atoms were markedly segregated on the surface, and a sharp $p(3 \times 1)$ LEED pattern appeared [3,4]. An interesting fact is that the reconstructed $p(3 \times 1)$ Pt–Rh(100)/O surface has remarkable catalytic activity for the reaction of $NO + H_2$ [5,6]. It was proved that very similar reconstructive activation is brought about on a series of bimetallic surfaces of Rh/Pt(100), Pt/Rh(100), Rh/Pt(110), and Pt/Rh(110), and these surfaces have almost equal catalytic activity for $NO + H_2$ reaction [3–10]. (In this paper, the alloy is expressed as Pt–Rh and the bimetal as Pt/Rh.)

In this paper, we discuss the structure of these activated alloy and/or bimetallic surfaces.

2. Experimental

Single crystal sample disk was bridged between the two Ta wires (0.25-mm diameter) by spot welding and was heated by direct current through the Ta wires. Temperature was measured by using a chromel–alumel spot welded at the edge of the sample disk. The surfaces of Pt(100), Pt(110), Rh(100), Rh(110), and Pt–Rh(100) alloy (Pt/Rh = 0.25/0.75) disks were cleaned in an ultra-high vacuum (UHV) chamber. In the case of Rh(100) and Rh(110) surfaces, the sample crystal was heated in O_2 (5×10^{-8} Torr) at 760–780 K for 20 min. Then, it was followed by repeating the Ar–ion sputtering and annealing at 1000–1200 K. Pt(100) and Pt(110) surfaces were cleaned by repeating the Ar–ion sputtering and annealing at 1100 K in UHV. After the annealing, the Pt(100) surface gave a (5×20) LEED pattern and the Pt(110) gave a $p(1 \times 2)$ LEED pattern.

Bimetallic surfaces were prepared by electrochemical deposition of Pt or Rh atoms on a desired Rh or Pt single crystal surface in an attached small volume cubic chamber. When the sample is transferred into the cubic cell, the cubic chamber is perfectly separated from the main UHV chamber by tight contact of a conic-shaped sample holder head so that one can carry out high pressure experiments up to 1 atm pressure in the small-volume cubic chamber. The cubic reactor was filled with 1 atm of highly pure Ar gas. Then, an electrochemical quartz cell filled with 0.05 M H_2SO_4 solution containing a certain concentration of Pt or Rh ion was lifted in the cubic cell to make a meniscus contact between the solution surface and one side of the crystal surface. After the electrochemical deposition of desired amount of Pt or Rh, the crystal disk was washed with highly pure water and was transferred back to the UHV main chamber for the characterization by LEED and AES. Details of the electrochemical deposition were described elsewhere [11,12].

Temperature programmed reaction (TPR) was performed by raising the temperature in a flow of a mixture of NO and H_2 (typically 5.8×10^{-9} Torr of NO and 1.6×10^{-8} Torr of H_2), and the reaction was monitored by a quadrupole mass spectrometer.

3. Results and discussion

3.1. $NO + H_2$ reaction on Pt(100), Pt(110), Rh(100), and Rh(110) surfaces

Catalytic activity of Pt(100), Pt(110), Rh(100), and Rh(110) surfaces were compared by raising the crystal temperature in a flow of a mixture of NO and H_2. When the reaction occurs in a steady state at a given temperature, the ratio of N_2 to NO undergoes reproducible change in raising and lowering the temperature.

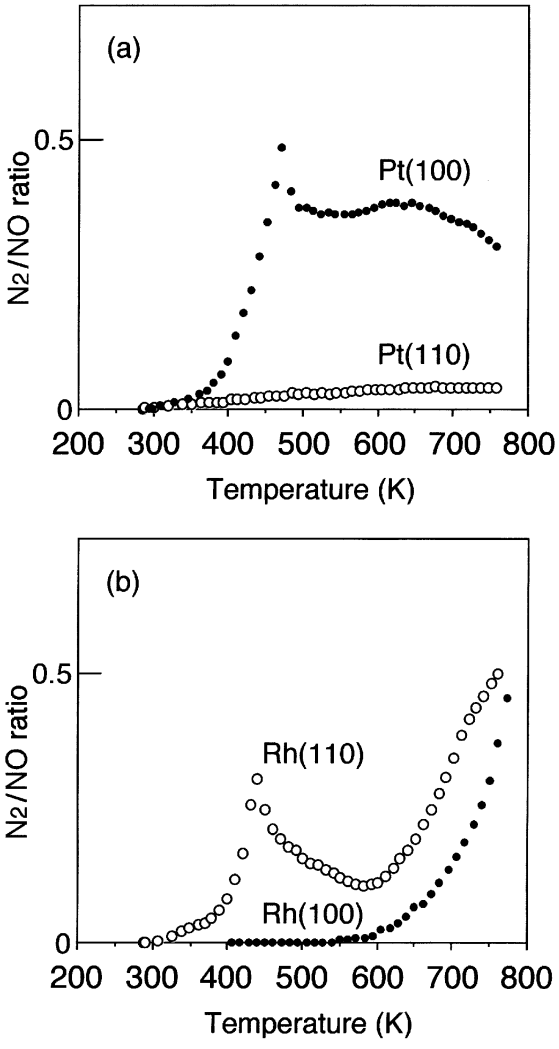

Fig. 1. Temperature programmed reaction of (a) Pt(100) and Pt(110) surfaces and (b) Rh(100) and Rh(110) surfaces by raising temperature in a flow of a mixture of $NO + H_2$.

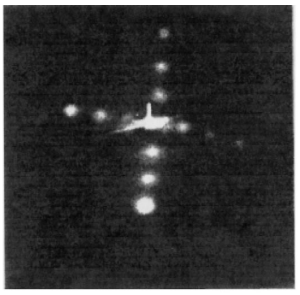

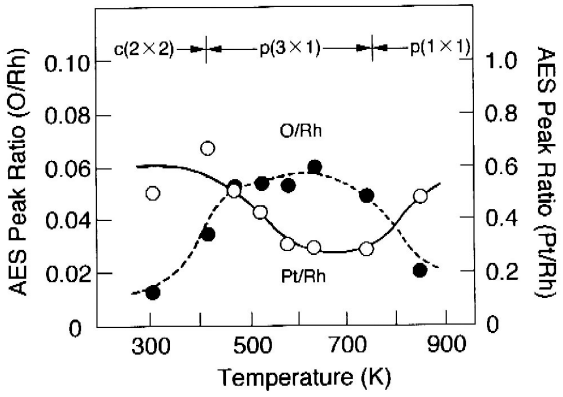

Fig. 2. Step-by-step heating of $Pt_{0.25}Rh_{0.75}(100)$ surface in 1×10^{-7} O_2 for 5 min. Segregation of Rh and p(3×1) reconstruction occur at temperature higher than ca. 400 K.

A Pt(100), surface is highly active for the reaction of $NO + H_2 \rightarrow 1/2N_2 + H_2O$, as shown in Fig. 1a, but a Pt(110) surface is almost inactive in the temperature range studied. It is known that when a Pt(100) is heated up in a flow of a mixture of $NO + H_2$, the ratio of N_2/NO has a peak at around 450 K but this peak does not appear in the cooling down process. Accordingly, the peak at around 450 K is not the catalytic reaction, and it is supposed to be a desorption mediated reaction of NO [13,14]. Similar noncatalytic emission of N_2 was also observed on Rh(110), as shown in Fig. 1b. A similar type of N_2 emission was observed in the TPD of adsorbed NO on Pd(110) and the mechanism for the emission of N_2 was precisely studied by measuring the spatial distribution of N_2 and NO [13,14]. Interestingly, the N_2 emitted with the desorption of NO from the Pd(110) surface takes ca. 38° off-normal to the surface in the [001] direction. But, it was proved that

the N_2 produced by the catalytic reaction takes $\cos\theta$ distribution. Using N^{15}, it was proved that the off-normal emission of N_2 is given by the reaction of desorbing NO molecules with N atoms, $NO + N \rightarrow N_2 + O$, on the Pd(110) surface, and therefore it was named as ''desorption mediated reaction'' [14].

The reaction on Rh(100) surface is very slow at temperatures lower than ca. 600 K, but is steeply promoted at higher than 600 K, which may indicate a high activation energy for the dissociation of NO on Rh(100) surface.

These results show that the catalytic reaction of $NO + H_2$ on Pt, as well as on Rh single crystal surfaces, sensitively depends on the crystallographic surface structures, and the activity sequence is Pt(100) ≫ Pt(110) and Rh(110) > Rh(110). In contrast, the catalytic reaction of $NO + H_2$ changes to entirely structure insensitive on the Pt/Rh bimetallic surfaces, as will be discussed in Section 3.2.

3.2. $NO + H_2$ reaction on Rh/Pt(100), Rh/Pt(110), Pt/Rh(100), and Pt/Rh(110) bimetallic surfaces

From a general viewpoint of the practical catalyst, structure-sensitive catalysis is undoubtedly a serious disadvantage. For example, in the case of the Pt and Rh catalyst, only a limited part of Pt and/or Rh will work as catalyst for the reaction of $NO + H_2$, and a large part of Pt

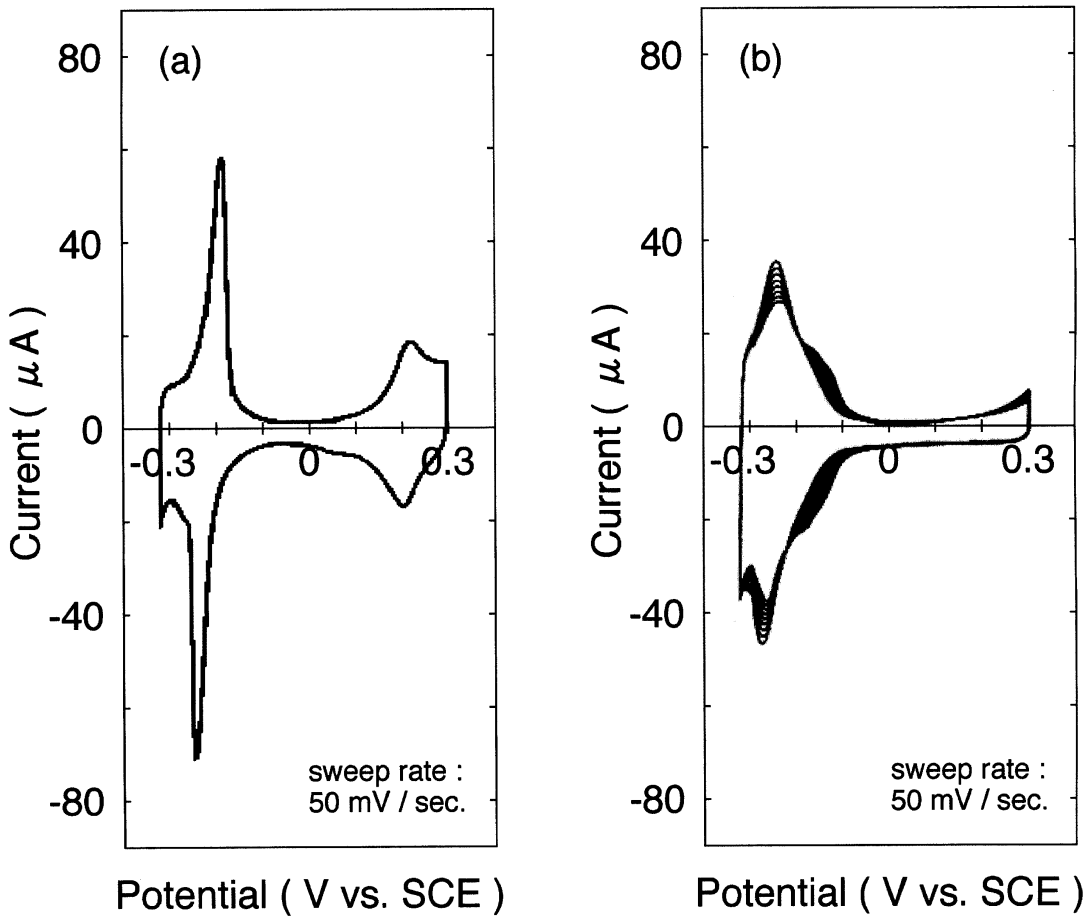

Fig. 3. (a) Cyclic voltammogram of a clean Rh(100) surface in a solution of 0.05 M H_2SO_4. (b) Cyclic voltammogram of a Pt deposited Rh(100) surface in a solution of 0.05 M H_2SO_4 containing 5×10^{-5} M of $PtCl_6^{2-}$.

or Rh does not work as the catalyst. Therefore, the role of Rh in the Pt/Rh three-way catalyst is a very interesting subject to understand. In order to gain an insight into the mechanism of Pt/Rh bimetallic catalyst, we studied first a $Pt_{0.25}Rh_{0.75}(100)$ alloy surface, and it was found that the alloy surface undergoes reconstructive activation during catalysis [3,4]. From this discovery, we intended to make clear the activation mechanism using such bimetallic surfaces as Rh/Pt(100), Rh/Pt(110), Pt/Rh(100), and Pt/Rh(110).

Pt/Rh alloy is a random alloy so that the $Pt_{0.25}Rh_{0.75}(100)$ surface is supposed to take a random distribution of Pt and Rh atoms. On the other hand, it was shown that the depth distribution of Pt and/or Rh is not uniform because the surface free energy depends on the composition. Accordingly, the surface composition of $Pt_{0.25}Rh_{0.75}(100)$ alloy changes by annealing temperature in UHV, but the compositional equilibration takes place rather slow at temperatures lower than ca. 950 K [15], which is quite consistent to an empirical rule for the rapid migration of surface atoms at higher than a half of melting temperature (0.5 T_m), Pt (T_m = 1997 K) and Rh (T_m = 2249 K). A depth distribution of a $Pt_{0.55}Rh_{0.45}$ needle annealed at ca. 973 K was shown by a layer-by-layer analysis by an FIM atom probe analysis, Pt is markedly enriched on the topmost layer but is depleted in the second layer [16]. It should be pointed out that the Pt and Rh composition for the layers deeper than the third is very close to the bulk composition. Tsong et al. [16] predicted that the Pt-fraction in the topmost layer will become higher as raising the annealing temperature, but it was experimentally contradicted by van Delft et al. [15], that is, the Pt-fraction of the $Pt_{0.25}Rh_{0.75}(100)$ surface monotonously decreases as raising the annealing temperature from ca. 950 to 1400 K.

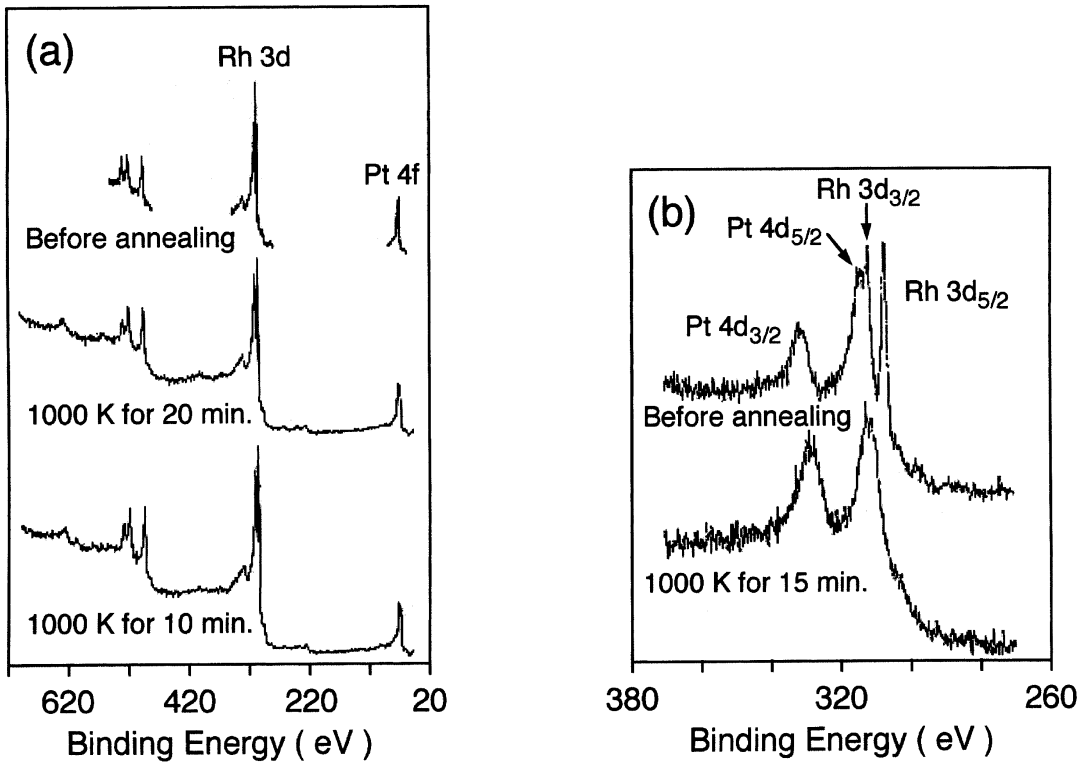

Fig. 4. XPS spectra showing thermal stability of bimetallic surfaces in UHV. (a) Pt deposited Rh(100). (b) Rh deposited Pt(100).

These results indicate that the surface composition of Pt–Rh alloy and Pt/Rh bimetallic surfaces will not rapidly change at lower than 950 K, even if the composition is not in equilibrium. This is very important because the catalytic reaction is usually performed in a temperature range of 450–700 K, which is far lower than the critical temperature of 950 K. In contrast to this expectation, however, it was found that the surface composition of Pt–Rh alloy [4] as well as of bimetallic surfaces [6] is changed during catalysis, where Rh atoms are readily extracted onto the topmost layer by reacting with oxygen even at 400 K.

When Rh atoms were extracted from the second layer by reacting with oxygen, the $Pt_{0.25}Rh_{0.75}(100)$ surface gave a clear $p(3\times1)$ LEED pattern, as shown in Fig. 2 [4,6,17]. It is worth noting that the $p(3\times1)$ surface has a constant Pt/Rh ratio and is readily changed to the $p(1\times1)$ pattern by keeping the ratio of Pt/Rh at room temperature (RT) by exposing to H_2 [6,12,17]. Taking account of the fact that Pt and Rh do not migrate on the surface at RT, the $p(1\times1)$ surface keeps an ordered array of Pt and Rh atoms of the $p(3\times1)$ structure over the (100) lattice structure. Based on these results, an STM image for the $p(3\times1)$ Pt/Rh(100)/O alloy surface was first observed by us [18].

When a Pt-enriched clean $Pt_{0.25}Rh_{0.75}(100)$ surface is heated in O_2, the $p(3\times1)$ LEED pattern appears after a certain induction time. Once the $p(3\times1)$ structure is established, the $p(1\times1)$ surface obtained by exposing to H_2 is readily changed to the $p(3\times1)$ at RT in a short time by exposing to O_2. It is also confirmed that the induction time for the formation of the $p(3\times1)$ $Pt_{0.25}Rh_{0.75}(100)$ surface becomes shorter and shorter by increasing the Rh fraction on the surface. If the $p(3\times1)$ surface is accomplished by the segregation of Rh and followed array of Rh and Pt atoms, the $p(3\times1)$ surface will take a constant Pt/Rh ratio, as observed in Fig. 2, and the induction time may correspond to the time for the accumulation of the required amount of Rh atoms. Therefore, such surface reconstruction is caused by ''chemical restructuring'', where the compositional change is brought about by a chemical reaction [6,17].

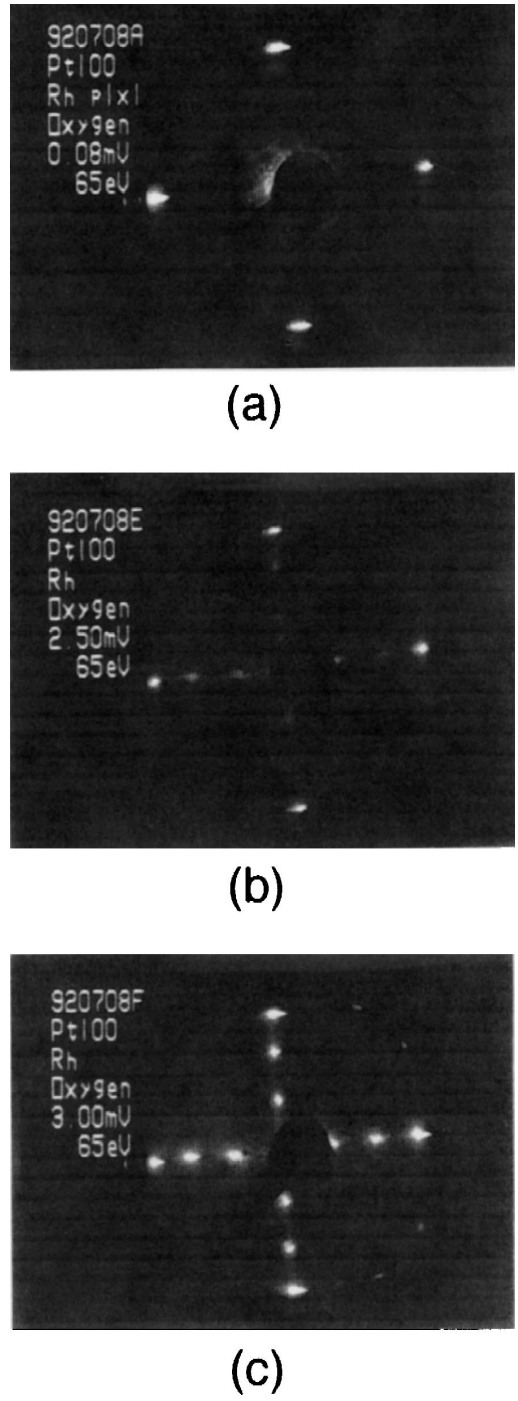

Fig. 5. Restructuring of (a) Rh deposited Pt(100) surface (θ_{Rh} = 0.4 ml) by annealing in 10^{-7} Torr of O_2 at (b) 340 and (c) 400 K.

The idea of chemical restructuring was more clearly confirmed on the two bimetallic surfaces, one is an Rh-deposited Pt(100) surface and the other is a Pt-deposited Rh(100) surface. The desired amount of Rh or Pt atoms was electrochemically deposited on a clean surface of Pt(100) or Rh(100) by repeating the cyclic potential sweep in H_2SO_4 solution. Fig. 3a shows a cyclic voltammogram of a clean Rh(100) surface in a solution of 0.05 M H_2SO_4 and Fig. 3b is that of a Pt deposited Rh(100) surface in a solution of 0.05 M H_2SO_4 containing 5×10^{-5} M of $PtCl_6^{2-}$. Characteristic hydrogen adsorption and desorption peaks that appeared on the clean Rh(100) surface at -0.26 and -0.19 V (SCE) are markedly suppressed by depositing Pt atoms. It is worth noting that the oxygen wave observed at a higher potential region on the clean Rh(100) surface disappears on the Pt deposited Rh(100) surface in the potential range scanned [17]. After the deposition, the bimetallic surface was washed by replacing the solution with ultra-pure water and then, the sample crystal was transferred back into the main UHV chamber for characterization.

XPS spectra for an as-deposited Pt/Rh(100) surface, the surface annealed at 1000 K for 20 min and that of subsequently annealed at 1050 K for 10 min are shown in Fig. 4a. It is clear that the Pt deposited Rh(100) surface is quite stable in UHV at a temperature as high as 1050 K. Contrary to this, Rh-layer on Pt(100) is not so stable, which undergoes rapid diffusion into the bulk, as shown in Fig. 4b, where the Rh atoms are perfectly dissolved into the bulk at 1000 K for 15 min.

It should be emphasized that the stability of the bimetallic surfaces is quite different in O_2 or NO. That is, when a Rh deposited Pt(100) surface ($\theta_{Rh}=0.4$ ml) was heated in O_2 of 1×10^{-7} Torr. A streaky LEED pattern appeared at 340 K and it changed to a very sharp $p(3\times1)$ LEED pattern at 400 K, as shown in Fig. 5. We supposed that the structure of this $p(3\times1)$ Rh/Pt(100)/O surface is the same as that of the $p(3\times1)$ Pt–Rh(100)/O alloy surface formed at ca. 450 K by annealing in O_2.

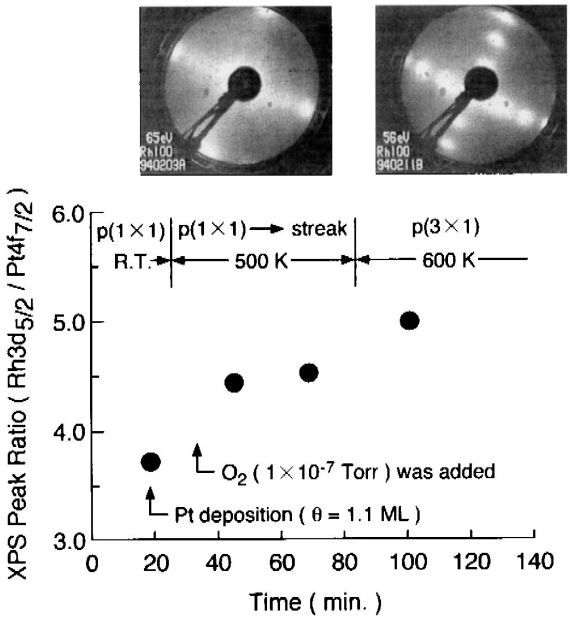

Fig. 6. Segregation of Rh on a Pt/Rh(100) ($\theta_{Pt}=1.1$ ml) by raising temperature in 10^{-7} Torr of O_2.

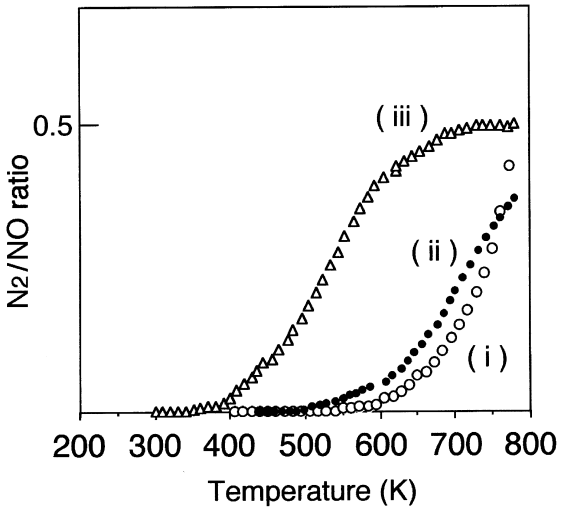

Fig. 7. Catalytic activity of (i) Rh(100), (ii) Pt/Rh(100) annealed at 1000 K, and (iii) p(3×1) Pt/Rh(100)/O surfaces by raising temperature in a flow of a mixture of 1×10^{-6} Torr of NO and 2×10^{-6} Torr H_2.

On the other hand, when a Pt/Rh(100) surface of ca. 1.1 ml of Pt was heated in O_2 of 1×10^{-7} Torr, a remarkable segregation of Rh was brought about at 500 K, as shown in Fig. 6, and a p(3 × 1) LEED pattern appears in subsequent annealing in O_2 at 600 K. Taking account of the fact that the Pt/Rh(100) surface is stable in UHV even at 1050 K, as shown in Fig. 4a, this Rh segregation and the following reconstruction are undoubtedly caused by the chemical restructuring. These phenomena are in good agreement with the longer induction time for p(3 × 1) restructuring on the Pt enriched Pt–Rh 100) alloy surface.

Taking account of the fact that the amount of Pt atoms deposited on the Pt/Rh(100) surface is ca. 1.1 ml, the extraction of a certain amount of Rh may take place by replacing Rh in the second layer with the Pt atoms. if this is the case, the formation of the p(3 × 1) surface is brought about by the chemical restructuring of the top two layers so that the second layer is enriched with Pt [17].

The most interesting fact is that the p(3 × 1) reconstructed surfaces of Pt–Rh(100) alloy, Rh/Pt(100), and Pt/Rh(100) are highly active for the redox reaction, that is, the LEED pattern change of the p(1 × 1) ↔ p(3 × 1) is readily conducted by exposing to H_2 or O_2 at RT, and the formation of such redox active surface may be responsible for the prominent catalytic activity of the Pt/Rh bimetallic catalyst for the reaction of $NO + H_2$. As shown in Fig. 7, Rh(100), as well as a Pt/Rh(100) surface annealed at 1000 K for 3 min in UHV, is not so active but the p(3 × 1) Pt/Rh(100)/O surface prepared by annealing in oxygen has a remarkable activity for the reaction of $NO + H_2$.

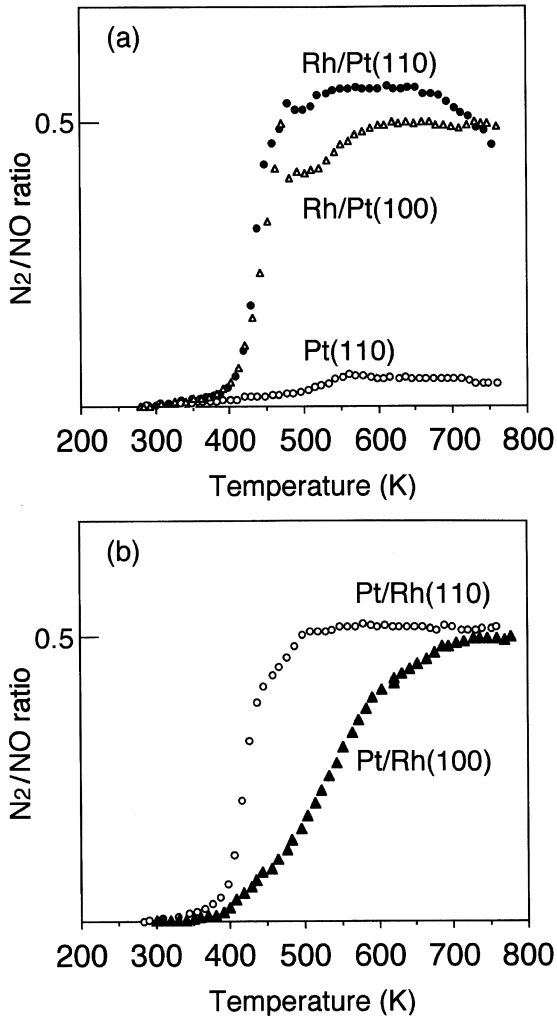

Fig. 8. Catalytic activity of the reconstructed bimetallic surfaces. (a) p(3×1) Rh/Pt(100)/O and c(2×2) Rh/Pt(110)/O. (b) p(3 ×1) Pt/Rh(100)/O and c(2×4) Pt/Rh(110)/O.

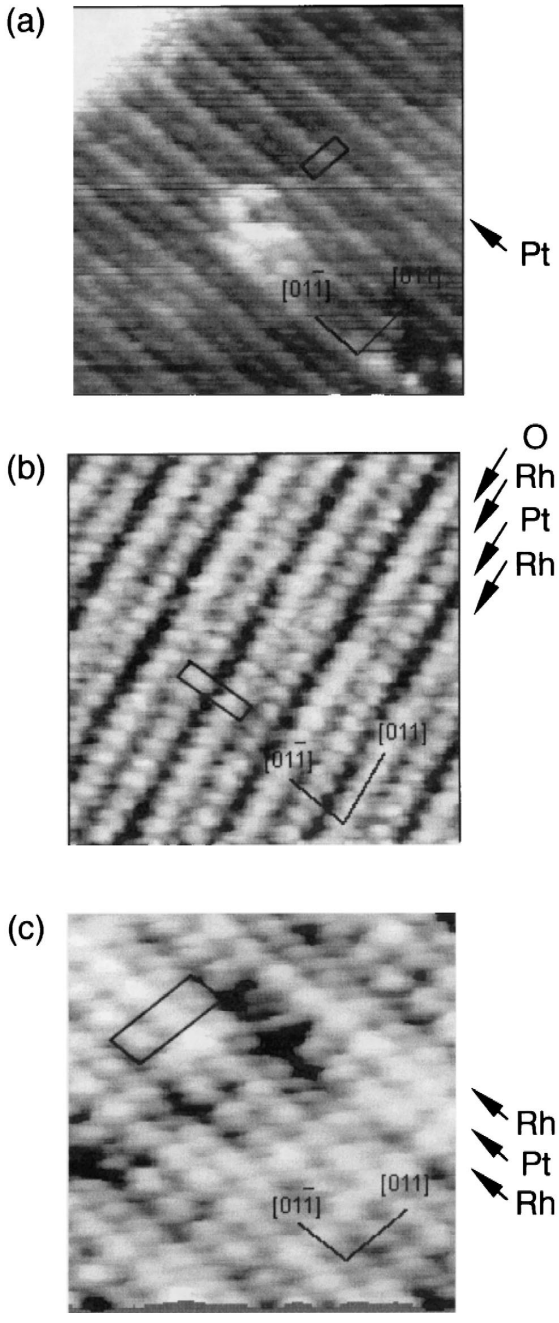

Fig. 9. Three STM images for a p(3×1) Pt/Rh(100)/O surface depending on the tip condition. (a,b) Either the Pt rows or Rh rows are seen. (c) Pt and Rh atoms forming a (100) lattice are seen.

Rh/Pt(110) and Pt/Rh(110) surfaces are also activated by annealing in O_2, that is, the surfaces undergo restructuring with the segregation of Rh atoms by the reaction with oxygen. As mentioned above, a clean Pt(110) surface is inactive for the reaction of $NO + H_2$, but a bimetallic Rh/Pt(110) surface was markedly activated by annealing in O_2, as shown in Fig. 8, where the activated Rh/Pt(110)/O surface gave a c(2 × 2) LEED pattern and was changed to a p(1 × 2) by exposing to H_2. In contrast, the activation of a bimetallic Pt/Rh(110) surface required the segregation of Rh by annealing in O_2 at 760 K, where a c(2 × 4) LEED pattern appeared. The catalytic activity was markedly enhanced by the formation of the c(2 × 4) reconstructed surface.

It should be emphasized that these reconstructed surfaces of c(2 × 2) Rh/Pt(110)/O and c(2 × 4)Pt/Rh(110)/O have almost equally

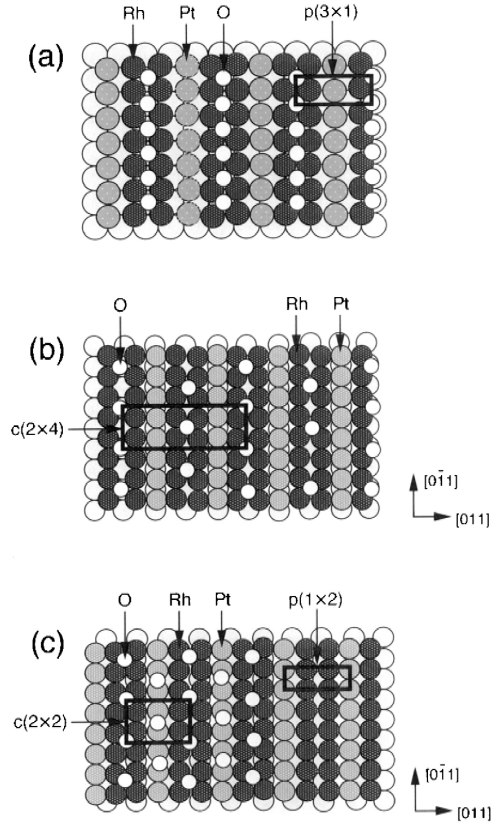

Fig. 10. Model structures for the reconstructed active surfaces of (a) p(3×1) Pt/Rh(100)/O, (b) c(2×4) Pt/Rh(110)/O, and (c) c(2×2) Rh/Pt(110)/O.

high catalytic activities for the reaction of NO $+ H_2$, and a noticeable fact is that the catalytic activities of the c(2 × 2) Rh/Pt(110)/O and c(2 × 4) Pt/Rh(110)/O surfaces are almost equal to that of the p(3 × 1) Rh/Pt(100)/O surface shown in Fig. 8.

From these results, it is deduced that the c(2 × 2) Rh/Pt(110)/O, c(2 × 4) Pt/Rh(110)/O, p(3 × 1) Rh/Pt(110)/O and p(3 × 1) Pt/Rh(100)/O surfaces are restructured by the reaction of Rh with O_2, and this chemical restructuring is responsible for the activation of these bimetallic surfaces. If this is the case, an interesting question is why these reconstructed surfaces have an almost equal catalytic activity for the reaction of NO + H_2. We supposed that the restructuring of these surfaces may form the active sites having similar local structure. From this point of view, the p(3 × 1) Pt–Rh(100)/O alloy surface was precisely studied using STM [18]. Interestingly, the p(3 × 1) Pt–Rh(100)/O alloy surface gives three different STM images depending on the tip condition, as shown in Fig. 9, where the Pt as well as the Rh atoms can be seen in image (a) but the images of (b) and (c) reflect either Pt or Rh atoms.

Accordingly, we can deduce a suitable model for the p(3 × 1) surface such as shown in Fig. 10a, which is different from the model temporally proposed in Ref. [18]. If the c(2 × 4) Pt/Rh(110)/O and c(2 × 2) Rh/Pt(110)/O surfaces are composed of active sites having similar local structure as that of the p(3 × 1) surface, we can deduce suitable structures for the c(2 × 4) Pt/Rh(110)/O and c(2 × 2) Rh/Pt(110)/O surfaces such as those shown in Fig. 10b and c.

Based on a series of experiments on Pt–Rh(100) alloy and Pt/Rh(100), Pt/Rh(110), Rh/Pt(100), and Rh/Pt(110) bimetallic surfaces, we could conclude that formation of active sites a common structure of Pt and Rh atoms on Pt/Rh bimetallic surfaces during catalysis is responsible for the prominent catalytic activity of this catalyst for removing NO_x, CO, and hydrocarbons in the automotive exhaust gas. In other words, ''a well-developed or -optimized catalyst will be structure-insensitive because they would provide the highest density of active sites, which is an important requisite for the perfectly improved catalyst''.

Acknowledgements

This work was supported by a Grant-in-Aid for Scientific Research (11640590) of the Ministry of Education, Science, and Culture of Japan. One of the authors (K.T.) also appreciates support in part by a project of the High-Tech Research Center of Saitama Institute of Technology.

References

[1] S.R. Bare, D.R. Strongin, G.A. Somorjai, J. Phys. Chem. 90 (1986) 4726.
[2] D.R. Strongin, S.R. Bare, G.A. Somorjai, J. Catal. 103 (1987) 289.
[3] H. Hirano, T. Yamada, K. Tanaka, J. Siera, B.E. Nieuwenhuys, Surf. Sci. 222 (1989) L804.
[4] H. Hirano, T. Yamada, K. Tanaka, J. Siera, B.E. Nieuwenhuys, Vacuum 41 (1990) 134.
[5] A. Sasahara, H. Tamura, K. Tanaka, J. Phys. Chem. 100 (1996) 15229.
[6] H. Tamura, K. Tanaka, Langmuir 10 (1994) 4530.
[7] T. Yamada, H. Hirano, J. Siera, B.E. Nieuwenhuys, K. Tanaka, Surf. Sci. 226 (1990) 1.
[8] A. Sasahara, H. Tamura, K. Tanaka, Catal. Lett. 28 (1994) 161.
[9] H. Tamura, A. Sasahara, K. Tanaka, Catalysis and automotive pollution control III, in: Stud. Surf. Sci. Catal. 96 Elsevier, 1995, pp. 229–236.
[10] A. Sasahara, H. Tamura, K. Tanaka, J. Phys. Chem. B 101 (1997) 1186.
[11] M. Taniguchi, E.K. Kuzembaev, K. Tanaka, Surf. Sci. Lett. 290 (1993) L711.
[12] K. Tanaka, M. Taniguchi, Top. Catal. 1 (1994) 95.
[13] M. Ikai, K. Tanaka, Surf. Sci. 357–358 (1996) 781.
[14] M. Ikai, K. Tanaka, J. Phys. Chem. B 203 (1998) 8279.
[15] F.C.M.J.M. van Delft, B.E. Nieuwenhuys, J. Siera, R.M. Wolf, Surf. Sci. 264 (1992) 435.
[16] T.T. Tsong, D.M. Ren, M. Ahdam, Phys. Rev. B 38 (1988) 7428.
[17] H. Tamura, A. Sasahara, K. Tanaka, J. Electroanal. Chem. 381 (1995) 95.
[18] Y. Matsumoto, Y. Okawa, T. Fujita, K. Tanaka, Surf. Sci. 355 (1996) 109.